JSC-08585

NASA TECHNICAL MEMORANDUM

NASA TM X-58113
January 1974

EFFECTS OF SELECTED TRAJECTORY PARAMETERS ON WEIGHT TRENDS IN THE SHUTTLE THERMAL PROTECTION SYSTEM

NATIONAL AERONAUTICS AND SPACE ADMINISTRATION

LYNDON B. JOHNSON SPACE CENTER

HOUSTON, TEXAS 77058

NASA TM X-58113

EFFECTS OF SELECTED TRAJECTORY PARAMETERS ON WEIGHT TRENDS IN THE SHUTTLE THERMAL PROTECTION SYSTEM

Donald M. Curry, James W. Tolin, Jr., and Winston D. Goodrich
Lyndon B. Johnson Space Center
Houston, Texas 77058

CONTENTS

TABLES

FIGURES

EFFECTS OF SELECTED TRAJECTORY PARAMETERS ON WEIGHT TRENDS IN THE SHUTTLE THERMAL PROTECTION SYSTEM

By Donald M. Curry, James W. Tolin, Jr.,
and Winston D. Goodrich
Lyndon B. Johnson Space Center

SUMMARY

A computer program was developed to compute thermal protection system weights for given input entry conditions. An empirically derived heating model that includes laminar, transitional, and turbulent heating correlations as functions of angle of attack, free-stream velocity, and free-stream density was obtained from a first-order extrapolation of wind tunnel data to flight conditions. A unit area weight correlation for a reusable surface insulation was developed as a function of local heat load and entry time. The heating model, the thermal protection system correlation methodology, and a four-degree-of-freedom trajectory integration program were combined to develop a thermal protection system trajectory computer program. Analytical studies were performed for a typical delta wing Space Shuttle Orbiter to predict the thermal protection system weight trends with entry parameter variations. The results of this specific study are described.

INTRODUCTION

The design and development of a minimum-weight thermal protection system (TPS) for the Space Shuttle are required to minimize weight and cost and to allow maximum payload capability. However, this development requires an optimum blend of material selection and system design, and this, in turn, is strongly dependent on the severity and duration of the aerothermodynamic environment experienced by the TPS. The procedure for obtaining an optimum blend of the design parameters that minimize TPS weight within specific operational constraints is described in the following paragraphs. Emphasis is placed on the gross trends of the results as the operational constraints are allowed to vary, rather than on the absolute value of the resulting TPS weights. The results of this study should not be applied to absolute TPS weights for vehicles that do not conform to the specific design methodologies used in this study.

To blend the technologies required to perform this study, a computer program was developed to determine the optimum entry trajectory in relation to the Space Shuttle TPS weight. The program can also be used to compute TPS weights for given input entry trajectories or for trajectories defined by non-TPS criteria such as equilibrium glide, acceleration limit, or other prescribed control logic.

To apply the TPS design and aerothermodynamic-environment prediction methodologies to the complete Shuttle/Orbiter, the outer surface area of a typical delta wing Space Shuttle Orbiter (JSC-040A) was divided into 20 surface panels. Because of the assumed symmetry of the vehicle and its environment, only one symmetrical half of the vehicle was necessary to perform this study.

An average surface heat transfer rate environment was specified for each panel. Laminar, transitional, and turbulent heat transfer rates were specified as functions of vehicle angle of attack, free-stream velocity, and free-stream density. These heating rates were obtained from a first-order extrapolation of normalized wind tunnel data to flight conditions. Increases in local heating rates due to transitional and turbulent boundary layers were computed as functions of the Reynolds number per meter behind a normal shock. Critical values of the Reynolds number per meter behind a normal shock causing the onset of transitional and fully turbulent flow were assigned to each surface panel. This environmental prediction procedure was sufficiently accurate for this study because the unit area TPS weight of a panel is proportional to the one-eighth power of the panel unit area heat load.

Unit area weight correlations for the reusable surface insulation (RSI) were developed as a function of local heat load and entry time. Weights of the surface coating and adhesive bond system were included in the TPS weight calculation procedure. A TPS computer program was used to calculate the RSI thickness required to maintain prescribed bondline temperature limits after the initiation of the entry phase.

This report describes the analytical heating model, TPS correlation methodology, and trajectory analyses that have been used in developing the TPS trajectory computer program.

SYMBOLS

A surface panel area, meters^2

c_p specific heat, joules/kilogram-kelvin

C_1	average slope of unit weight W/A curves (fig. 3)
$C_2(t)$	the abscissa intercept (fig. 3) for W/A values of zero
C_3, C_4	values defined in equation (12)
K	thermal conductivity, watts/meter-kelvin
Q	total heat, joules/meter^2
$\dot{q}$	heat flux rate, watts/centimeter^2
Re	Reynolds number
T	temperature, kelvin
t	heating time, seconds
V	velocity, meters/second
W/A	weight of insulator per unit area, kilograms/meter^2
α	angle of attack, degrees
γ	flightpath angle, degrees
ε	emissivity
μ	viscosity, newton-second/meter^2
ρ	density, kilograms/meter^3
σ	Stefan-Boltzmann constant

Subscripts:

i	location
L	local
lam	laminar

ns	conditions behind normal shock
ns/m	per meter behind the normal shock
ref	reference, 0.305-meter-radius sphere
s	sea level
trans	transition
turb	turbulent
∞	free stream

ANALYTICAL METHODS

The TPS trajectory computer program contains aerothermodynamic heating relationships and TPS weight correlations that have been incorporated into a four-degree-of-freedom trajectory computer program. The assumptions used in these analyses and their validation are discussed in the following sections.

Aerothermodynamic Heating Methodology

The outer surface area of a typical delta wing Space Shuttle Orbiter configuration was divided into 20 panels (fig. 1). The areas and average aerodynamic heating data for each of the 20 panels are given in table I. The heating data given in table I represent laminar heating rates normalized by the stagnation point heating rate on a .305-meter-radius sphere. For the purpose of this study, these heating rates were obtained from test data that were averaged over the areas occupied by the panels. Transitional and fully turbulent boundary layer heating rates are presented as a function of the Reynolds number behind a normal shock. This reference Reynolds number was used in an effort to account for the effects of real gas flow on the flow field at flight conditions. Critical values of the Reynolds number from the onset of transitional flow have been approximated from limited turbulent flow data on the Shuttle (ref. 1).

The heating rates and temperatures on any one panel will be determined by the state of the boundary layer (i.e., laminar or turbulent), the angle of attack, and the free-stream density and velocity. Laminar heating rates are computed as

$$\dot{q}_{lam} = \left(\frac{\dot{q}_{lam}}{\dot{q}_{ref}}\right)\dot{q}_{ref} \tag{1}$$

where values of $\dot{q}_{lam}/\dot{q}_{ref}$ are obtained from the data in table I and $\dot{q}_{ref}$ from reference 2.

$$\dot{q}_{ref} = 19\ 974\sqrt{\frac{\rho_\infty}{\rho_s}}\left(\frac{V_\infty}{7925}\right)^{3.15} \tag{2}$$

When the Reynolds number per meter behind the normal shock $Re_{ns/m}$ exceeds the value of $\left(Re_{ns/m}\right)_{turb}$ on a given surface panel, the heating rate is assumed to be that from a turbulent boundary layer and is computed as

$$\dot{q}_{turb} = \left(\frac{\dot{q}_{lam}}{\dot{q}_{ref}}\right)\left(\frac{\dot{q}_{turb}}{\dot{q}_{lam}}\right)\dot{q}_{ref} \tag{3}$$

where $\dot{q}_{lam}/\dot{q}_{ref}$ is obtained from table I, $\dot{q}_{ref}$ is computed with equation (2), and the approximation for $\dot{q}_{turb}/\dot{q}_{lam}$ is represented by

$$\left(\frac{\dot{q}_{turb}}{\dot{q}_{lam}}\right) = 2.5\left[\frac{Re_{ns/m}}{\left(Re_{ns/m}\right)_{turb}}\right]^{0.3} \tag{4}$$

$$\left(\frac{\dot{q}_{turb}}{\dot{q}_{lam}}\right) = 2.5\left[\frac{Re_{ns/m}}{1.5\left(Re_{ns/m}\right)_{trans}}\right]^{0.3} \qquad (5)$$

When the computed Reynolds number per meter behind the normal shock is between the values of $\left(Re_{ns/m}\right)_{trans}$ and $\left(Re_{ns/m}\right)_{turb}$, the boundary layer is transitional; and the heating rates can be presented by a linear interpolation between the laminar and turbulent heating rates.

$$\dot{q}_{trans} = \dot{q}_{lam} + \left(\dot{q}_{turb} - \dot{q}_{lam}\right)\left[\frac{Re_{ns/m} - \left(Re_{ns/m}\right)_{trans}}{\left(Re_{ns/m}\right)_{turb} - \left(Re_{ns/m}\right)_{trans}}\right] \qquad (6)$$

where $\dot{q}_{lam}$ and $\dot{q}_{turb}$ are computed from equations (1) and (3). For example, the values of $\left(Re_{ns/m}\right)_{trans}$ and $\left(Re_{ns/m}\right)_{turb}$ from table I for panel 1 are 108 000 and 162 000, respectively.

The trajectory computer program incorporates an option for selecting one of two methods for computing the Reynolds number behind a normal shock. In one case, the Reynolds number is computed as

$$Re_{ns/m} = \frac{\rho_{ns}V_{ns}}{\mu_{ns}} = \frac{\rho_{\infty}V_{\infty}}{\mu_{ns}} \qquad (7)$$

where the viscosity μ of the air is calculated behind the normal shock by using equilibrium real gas thermodynamic and transport properties. If knowledge of the flow properties behind the normal shock is not available, the second program option is used to compute the Reynolds number for use in the heating rate calculations of equations (4), (5), and (6). In this case, the Reynolds number per meter behind the normal shock is approximated by the relationship

$$Re_{ns/m} = 172\left(\frac{\rho_{\infty}V_{\infty}^{2}}{\sqrt{\dot{q}_{ref}}}\right)^{1.5} \qquad (8)$$

Equilibrium panel surface temperatures can now be computed from the relationship

$$T_i = \left(\frac{\dot{q}_i}{\sigma\varepsilon}\right)^{0.25} \tag{9}$$

where $\dot{q}_i$ is the panel heating rate. Finally, panel heat loads Q_i are obtained from

$$Q_i = \int_0^t \dot{q}_i \, dt \tag{10}$$

Weight Correlation Methodology

The TPS weights are dependent on the aerothermodynamic heating environment (laminar/turbulent flow) and the entry trajectory (orbit altitude and inclination, entry range, and entry flightpath angle). To eliminate the necessity of performing detailed sizing of a TPS for each entry trajectory flown, a concise semiempirical method was developed to determine required RSI thickness over a wide range of entry trajectory variables. S. A. Mezines developed a similar technique (ref. 3) to estimate ablator weights. For an ablative slab subjected to a constant heat rate, Mezines found that a correlation which used total heat load Q and heating time t of the entry trajectory could be used to predict ablation TPS weights. Since the Shuttle/Orbiter entry guidance operates in a constant heating rate mode during the time of significant heating, the entry environment is similar to the constant heating test conditions in Mezines' analysis. Thus, the same correlation parameter $(Q_T t^3)^{1/8}$ was used to develop a TPS-RSI unit weight correlation for Orbiter entries.

Five Shuttle entry trajectories were used to develop a correlation of RSI unit weight as a function of heat load and entry time. These trajectories represented entry ranges of 6802 to 15 442 kilometers, trajectory entry times of 31 to 56 minutes, and total reference heat loads (0.305-meter-radius sphere) of 7.65×10^8 to 14.02×10^8 J/m^2. The RSI unit weight correlations were computed using pressure and temperature dependent properties (table II). For this study, the TPS configuration (fig. 2) consisted of RSI bonded to an aluminum structure and was thermally modeled as a three-layer system (RSI, adhesive bond, and aluminum). The model was assumed to be at 300 K at the start of entry with an adiabatic boundary condition imposed on the aluminum back surface during entry. Curves of RSI unit weight as a function of $(Q_L t^3)^{1/8}$ were developed for the trajectories ummarized in table III. By using a TPS weight computation program (ref. 4), optimized RSI thickresses were calculated with a 442 K maximum aluminum structure temperature constraint and an RSI minimum material thickness of 0.648 centimeter. Mezines' correlation parameter $(Q_L t^3)^{1/8}$ reduces the RSI unit weight data to a series of almost straight lines from which an empirical relationship was developed.

The basic relationship developed from these curves is

$$(W/A)_{RSI} = C_1\left(Q_L t^3\right)^{1/8} + C_2(t) \tag{11}$$

where C_1 represents an average slope of the unit weight W/A curves plotted in figure 3 and $C_2(t)$ represents a relationship involving only the time from entry interface to the point at the end of entry when the reference heating rate is 22.7 kW/m^2. Assuming that

$$C_2(t) = C_3\left(t - t_0\right) + C_4 \tag{12}$$

where $C_2(t)$ is defined as the abscissa intercept for W/A values of zero, combining equations (11) and (12) yields the basic relationship for predicting RSI unit weight

$$(W/A)_{RSI} = C_1\left(Q_L t^3\right)^{1/8} + C_3\left(t - t_0\right) + C_4 \tag{13}$$

Using the TPS model just described and the unit weight curves of figure 3, the following relationship was obtained

$$(W/A)_{RSI} = 0.25633\left(Q_L t^3\right)^{1/8} - \left(7.036 \times 10^{-3}\right)(t - 1200) - 24.4 \tag{14}$$

In computing W/A from equation (14), the minimum W/A value on any panel is limited to 1.528 kg/m^2 (0.648-centimeter minimum RSI thickness).

The total TPS weight for the Orbiter is determined by summing the weight of each surface panel as follows.

$$\text{Total TPS weight} = \sum_{i=1}^{20} A_i (W/A)_i \tag{15}$$

In addition to the RSI unit weight, surface-coating and adhesive-bond unit weights must be included in the total TPS weight calculation of equation (15).

Trajectory Analyses

Trajectory model.- The data presented in the subsequent sections were obtained by using a four-degree-of-freedom trajectory integration program that incorporated a closed-loop entry guidance method.

Down-range control is provided by modulating the roll angle, and cross-range control is provided by controlling the direction of the roll angle. The roll control logic is based on analytical range predictions and is divided into three phases: the constant heat rate phase, the equilibrium glide ranging phase, and the constant-g ranging phase.

The constant heat rate phase begins at 0.49 m/sec^2 and is used to stabilize the trajectory at pullout ($\gamma = 0$). This phase is terminated when the current velocity is less than 7620 m/sec. The equilibrium glide ranging phase computes the roll angle (based on flying an equilibrium glide profile) required to null the range errors. Control is transferred to the constant-g ranging phase when the current load factor is equal to the constant-load-factor level required to reach the target

(14.7 m/sec^2). The constant-g ranging phase computes the desired constant-g level required to null the range errors and converts the desired constant-g level into a roll angle command. Control is transferred to the transition logic at Mach 6.

The data are based on the JSC-040A delta wing Space Shuttle Orbiter aerodynamics and a weight of 63 502 kilograms. Although the JSC-040A is no longer the baseline configuration, it is a representative Orbiter delta configuration. The 1962 standard atmosphere was used for all analyses. The trajectories were targeted to the NASA John F. Kennedy Space Center.

Targeting.- The deorbit was nominally targeted to achieve the entry target line presented in figure 4. The deorbit attitudes were selected to provide the deorbit velocity increment along the local horizontal. The nominal entry range was selected for each case by biasing the entry range from the minimum achievable entry range. The minimum achievable entry range is based on either a 1644 K temperature limit at a point 12.5 percent aft of the nose on the underside centerline (panel 1) or on a 2.5g load-factor limit, whichever results in the longer entry range. The constant angle-of-attack entries are constrained by the temperature limit, and the variable angle-of-attack entries are constrained by the load-factor limit.

The nominal target is biased so that the nominal entry range is 1111 kilometers greater than the minimum achievable entry range. This bias was selected so that navigation, atmospheric, and aerodynamic dispersions will not result in temperature or load-factor constraint violations. The TPS weight, maximum load factor, and maximum panel 1 temperature are presented in figure 5 as a function of entry range for a typical set of entry conditions. The nominal entry range is presented in figure 6 as a function of orbit altitude and inclination for constant and variable angle-of-attack entry profiles. In general, the trend is for range to increase as orbit altitude and inclination increase; this trend reverses, however, at lower inclinations. The reversal is caused by the oblateness effect associated with entry latitude at low inclinations

RESULTS OF DELTA WING ORBITER STUDY

Results of the JSC-040A delta wing Space Shuttle Orbiter study are presented to show the effects of entry trajectory parameters on the TPS weight. The TPS includes an RSI characterized by a 1644 K surface temperature limit, except for the surface leading edges that have a higher temperature limit.

The TPS weight requirements are defined as a function of orbit inclination, orbit altitude, entry range, and entry flightpath angle. Data are presented for the constant and variable angle-of-attack entry profiles. These profiles were selected to minimize the TPS weight while providing a 2222-kilometer cross-range capability at 90° inclination. The TPS weights are based on the heating and TPS models discussed in the section entitled "Analytical Methods."

The effects of orbit inclination, orbit altitude, entry range, and entry flightpath angle are presented in figures 7 to 11 for the constant angle-of-attack entry profiles. Data are presented for orbit altitudes that vary from 185 to 1296 kilometers and for inclinations that vary from 28.5° to 140°. Figures 7 and 8 present TPS weight change as a function of orbit inclination and orbit altitude. The trend is generally as expected, with TPS weight increasing as inclination and orbit altitude increase; however, this trend reverses with lower inclination values. This is the same effect as that shown in figure 6.

The reference TPS weight was obtained by using an entry trajectory that deorbited from an apogee of 500 kilometers at 55° inclination. As shown in figure 7, reducing the orbit altitude at this inclination to 185 kilometers decreases the TPS weight by 352 kilograms, and increasing the orbit altitude to 926 kilometers increases the TPS weight by 590 kilograms. Increasing the inclination from 55° to 90° for a 500-kilometer orbit altitude increases the TPS weight by 340 kilograms.

Figure 9 presents normalized contours of TPS weight in the orbit inclination plane. It must be noted that these weights are for the nominal range and nominal flightpath angle. The TPS weight must be increased to compensate for dispersions in these parameters; however, the trends noted are valid.

Figure 10 illustrates the effect of entry range on the TPS weight for constant 30° angle-of-attack entry profiles. These data are for entries following deorbit from a 500-kilometer orbit altitude. The reference point for the entry range shown in figure 10 is the nominal range presented in figure 6. For a 55° orbit inclination, the sensitivity of TPS weight to entry range is approximately 0.50 kg/km.

Figure 11 presents the effect of variations in entry flightpath angle on the TPS weight for constant 30° angle-of-attack entry profiles. Data are presented for a 55° orbit inclination with 185- to 500-kilometer orbit altitudes.

The TPS weight for variable angle-of-attack entry profiles is presented as a function of orbit altitude, entry range, and entry flightpath angle in figures 12 to 14. Data are presented for inclinations of 55° and 90° and orbit altitudes of 185 to 926 kilometers.

Figure 12 shows the effect of inclination and orbit altitude on TPS weight. The reference zero weight point is for a 500-kilometer orbit at a 55° inclination. Entry at a 90° inclination for the same orbit altitude requires an additional 136 kilograms of TPS weight. Entry from a 185-kilometer orbit altitude requires 91 kilograms less TPS weight than entry from a 500-kilometer orbit at a 55° orbit inclination. Entry from a 926-kilometer orbit altitude requires 102 kilograms more TPS weight than entry from a 500-kilometer orbit altitude at this same inclination.

Figure 13 presents the effects of entry range on TPS weight for 55° and 90° orbit inclinations. The reference points for the entry range in these figures is the nominal entry range presented in figure 6(b). The sensitivity of TPS weight to range is approximately 0.71 kg/km for the variable angle-of-attack entry profile. Figure 14 illustrates the effect of entry flightpath angle on TPS weight for the variable angle-of-attack profile for a 55° orbit inclination and a 500-kilometer orbit altitude.

Table IV summarizes the weight sensitivity determined by this tradeoff study.

CONCLUSIONS

A computation procedure has been developed to combine an empirically derived heating model, thermal protection system (TPS) correlation methodology, and trajectory analysis. This program can be used to compute TPS weights for given input entry trajectories or for trajectories defined by non-TPS criteria such as equilibrium glide, acceleration limit, or a prescribed control logic.

This computation procedure was applied to the Lyndon B. Johnson Space Center 040A delta wing Orbiter to show the effects of entry trajectory parameters on the TPS weight trends, and TPS weight sensitivity coefficients were obtained.

Although the computation procedure developed cannot be used to predict exact TPS weights, gross trends of the TPS weight can be predicted as vehicle operational constraints are allowed to vary.

Lyndon B. Johnson Space Center
National Aeronautics and Space Administration
Houston, Texas, January 18, 1974
986-15-31-04-72

REFERENCES

1. Ried, R. C.; Goodrich, W. D.; Strouhal, G.; and Curry, D. M.: The Importance of Boundary Layer Transition to the Space Shuttle Design. Paper presented at the Boundary Layer Transition Specialist's Workshop, Aerospace Corp. (San Bernardino, Calif.), Nov. 3, 1971.

2. Detra, R. W.; Kemp, N. H.; and Riddell, F. R.: Addendum to Heat Transfer to Satellite Vehicles Re-Entering the Atmosphere. Jet Propulsion, vol. 27, no. 12, Dec. 1957, pp. 1256-1257.

3. Mezines, S. A.: A Rapid Technique for Estimating Ablative Heat Shield Weights from Plasma Jet Test Data. Vol. 21 of Thermal Design Principles of Spacecraft and Entry Bodies, Jerry T. Bevans, ed., Academic Press, 1969, pp. 203-223.

4. Williams, S. D.; and Curry, D. M.: Parameter Optimization — An Aid to Thermal Protection Design. J. Spacecraft Rockets, vol. 9, no. 1, Jan. 1972, pp. 33-38.

TABLE I.- AERODYNAMIC HEATING RATE DATA FOR THE MSC-040A DELTA WING ORBITER PANELS

Panel number (a)	Area, m^2	Angle of attack, deg	$\dot{q}_{lam}/\dot{q}_{ref}$	$\left(Re_{ns/m}\right)_{trans}$ (b)
1	24.8	30 53	0.221 .260	108 000
2	53.4	30 53	.091 .170	66 000
3	75.2	30 53	.065 .098	39 000
4	81	30 53	.065 .085	20 000
5	40.1	30 53	.051 .017	108 000
6	57.6	30 53	.031 .014	66 000
7	38.7	30 53	.020 .008	134 000
8	41.3	30 53	.005 .005	134 000
9	26.9	30 53	.026 .026	108 000
10	64.2	30 53	.008 .003	108 000
11	88.6	30 53	.009 .009	108 000
12	103.5	30 53	.004 .004	108 000
13	60.3	30 53	.020 .023	134 000
14	49.5	30 53	.104 .156	108 000
15	48.7	30 53	.065 .085	87 000
16	51.5	30 53	.033 .033	134 000
17	40.9	30 53	.020 .020	134 000
18	44.9	30 53	.021 .021	134 000
19	27	30 53	.025 .016	108 000
20	24	30 53	.020 .016	108 000

[a] See figure 1.

[b] Note: $\left(Re_{ns/m}\right)_{turb} = 1.5 \times \left(Re_{ns/m}\right)_{trans}$

TABLE II.- THERMAL PHYSICAL PROPERTIES

[Constant values: $\rho = 240\ kg/m^3$; $\varepsilon = 0.85$]

(a) Thermal conductivity

Temperature, K	Thermal conductivity K, W/m-K, at a pressure of				
	$1.337 \times 10^1\ N/m^2$	$1.337 \times 10^2\ N/m^2$	$1.337 \times 10^3\ N/m^2$	$1.337 \times 10^4\ N/m^2$	$1.013 \times 10^5\ N/m^2$
0	1.7068×10^{-4}	1.8992×10^{-4}	2.8007×10^{-4}	3.2093×10^{-4}	3.51×10^{-4}
422	2.1035	2.3078	3.1012	3.4017	3.726
644	2.7045	2.8968	3.5098	4.6878	5.229
1033	4.5075	4.6878	6.01	9.015	10.00
1367	6.7312	6.9115	10.217	14.06	15.63
1644	9.1352	9.3756	13.462	18.87	20.91

(b) Specific heat

Temperature, K	Specific heat C_p, J/kg-K
200	300
300	632
400	829
500	980
544	1101
700	1172
1000	1231
1400	1323
1605	1340

TABLE III.- THE JSC-040A ORBITER ENTRY TRAJECTORIES

Case	Trajectory time, min:sec	Down range, km	Maximum g	$\dot{q}_{ref}$ maximum, W/m^2	Q_{ref} total, J/m^2
1	40:40	9 692	1.5	9.56×10^5	10.80×10^8
2	34:00	6 947	1.5	15.39	8.62
3	36:20	7 875	1.5	11.70	9.45
4	55:40	15 442	1.5	7.20	14.02
5	31:20	6 802	2.2	17.09	7.65

TABLE IV.- WEIGHT SENSITIVITY OF THE TPS

Parameter	Constant angle of attack	Variable angle of attack
Nominal mission range,[a] km . . .	9112	6852
TPS weight sensitivity to entry range, kg/km	0.50	0.71
TPS weight sensitivity to orbit altitude,[b] kg/km	1.1	0.24
TPS weight sensitivity to inclination,[c] kg/deg	14.7	3.8
TPS weight sensitivity to entry flightpath angle,[a] kg/deg . . .	912	1263

[a]For 55° inclination, 500-km orbit altitude.

[b]Above 500-km orbit altitude for 55° inclination.

[c]Above 55° inclination for 500-km orbit altitude.

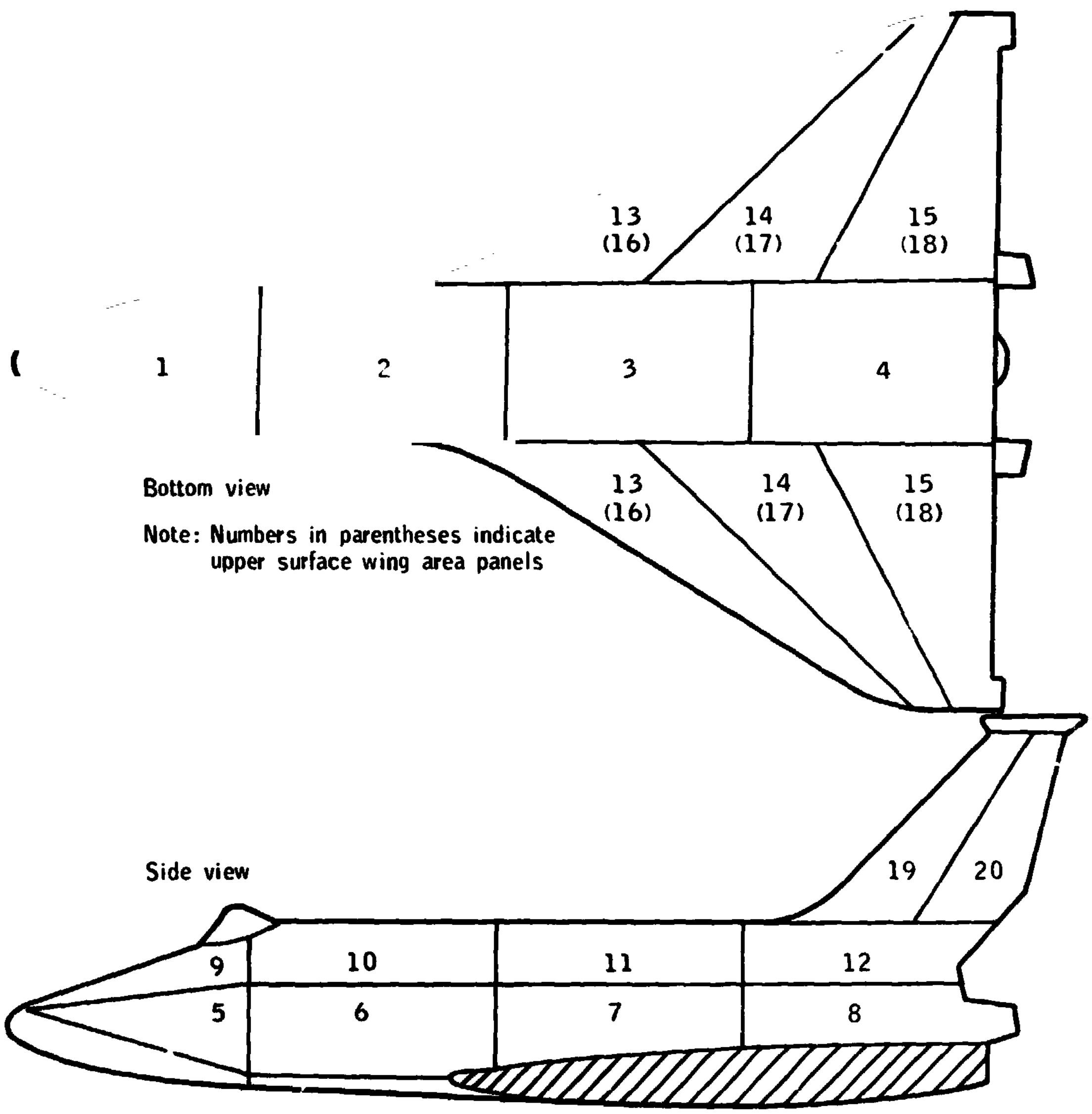

Figure 1.- Surface panels of a JSC-040A delta wing Orbiter.

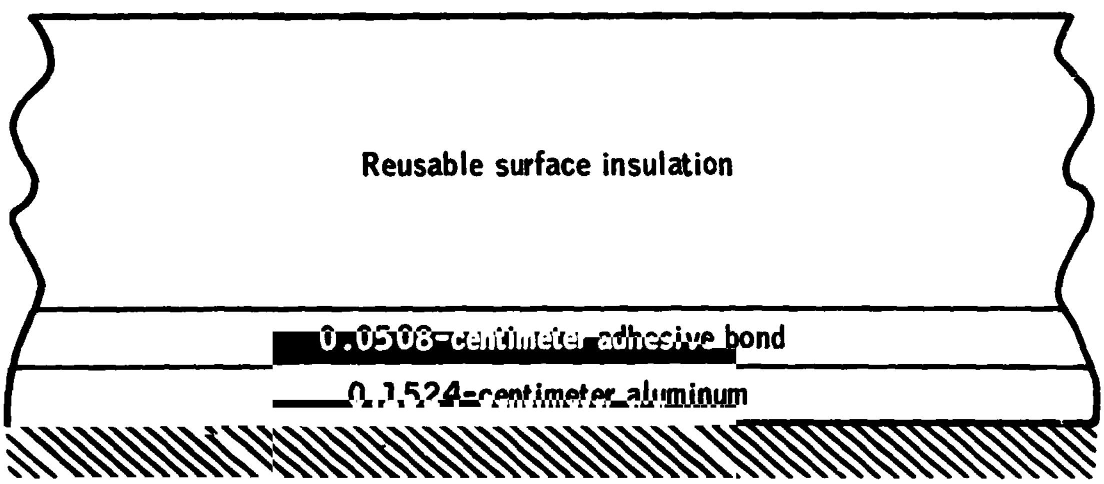

Figure 2.- Schematic of the TPS configuration.

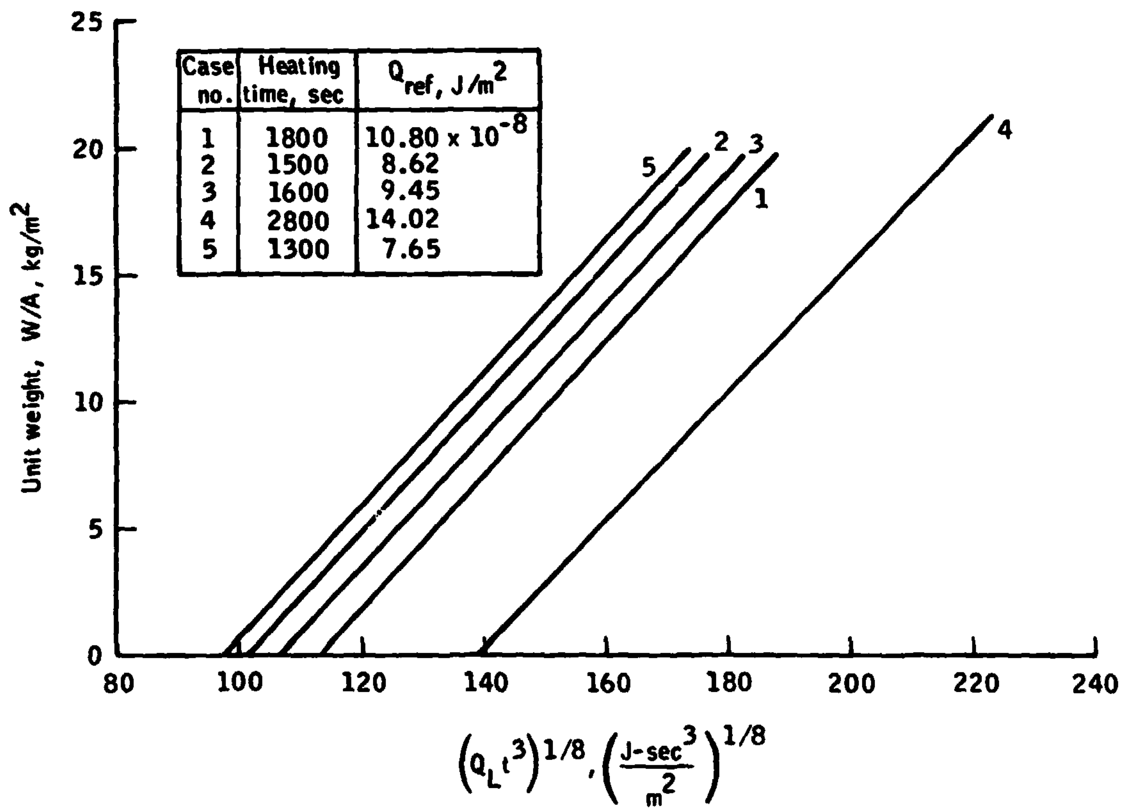

Figure 3.- The TPS unit weight as a function of total heat load and time.

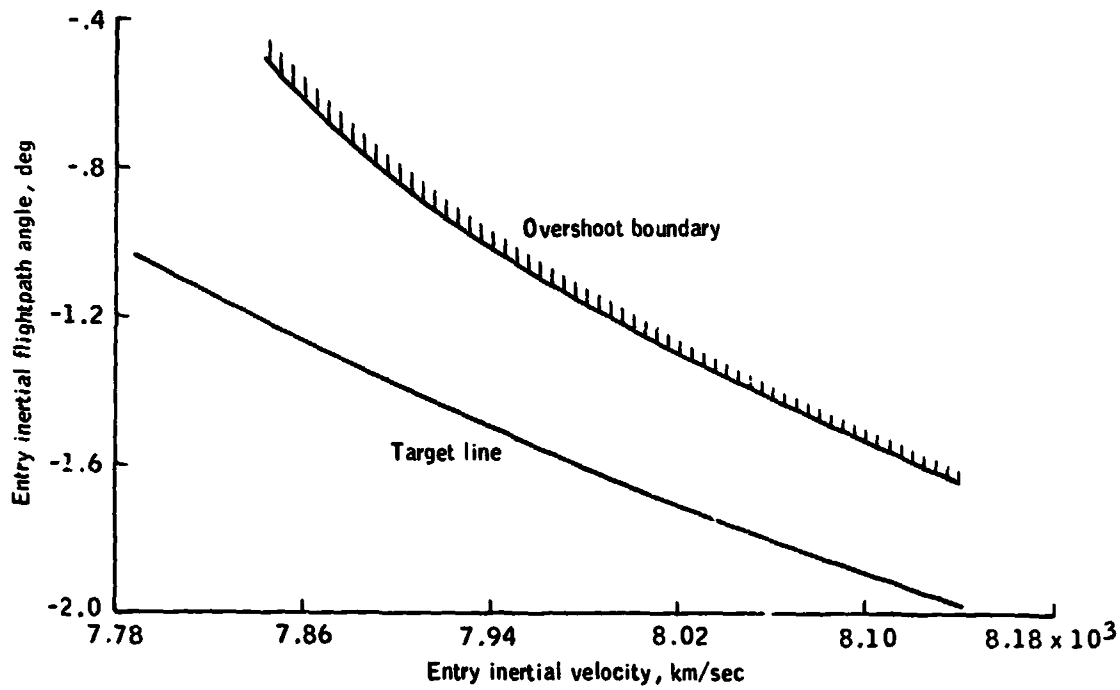

Figure 4.- Entry target line (inclination, 55°; angle of attack, 30°; 1962 standard atmosphere).

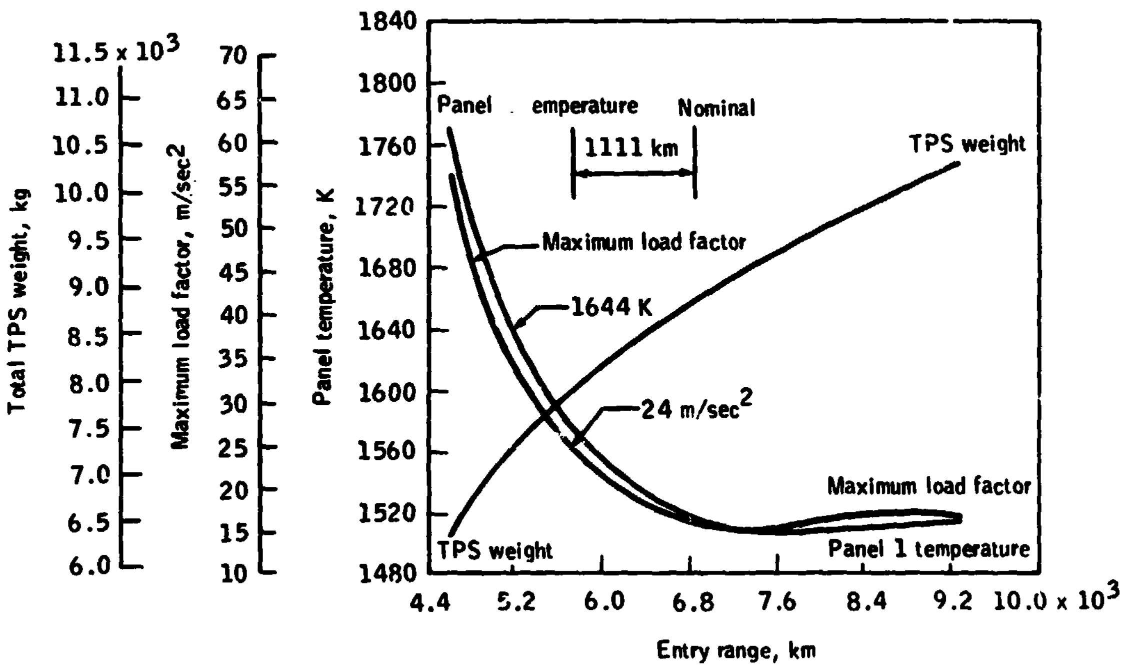

Figure 5.- Thermal protection system weight and maximum load factor compared to range for typical entry (inclination, 55°; variable angle of attack; orbit altitude, 500 kilometers).

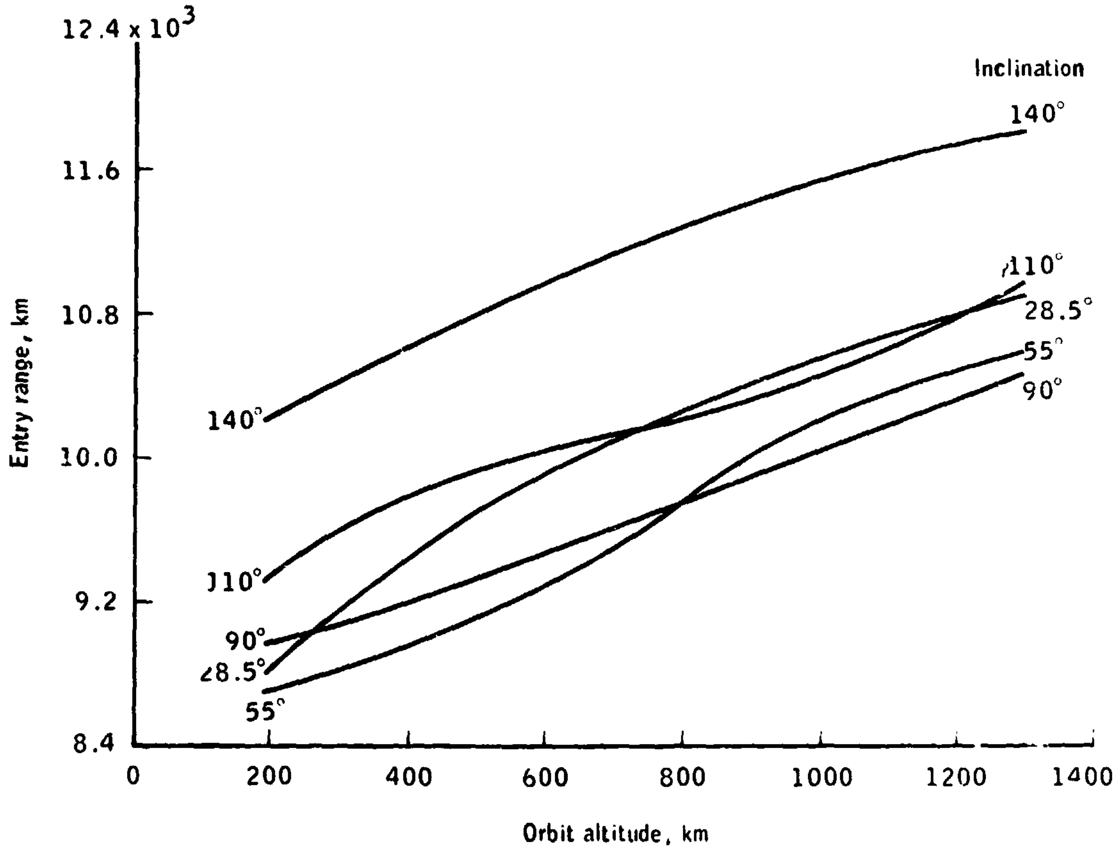

(a) Constant angle-of-attack entry profile.

Figure 6.- Nominal entry range.

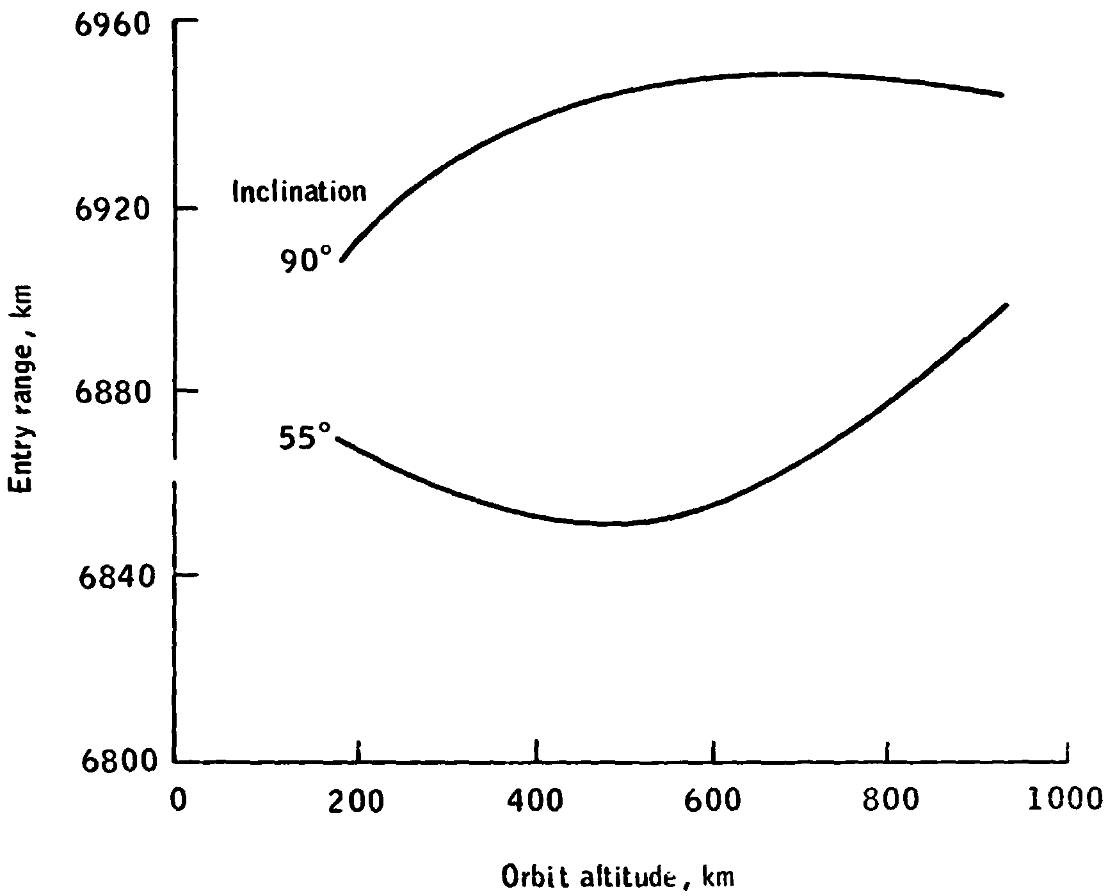

(b) Variable angle-of-attack entry profile.

Figure 6.- Concluded.

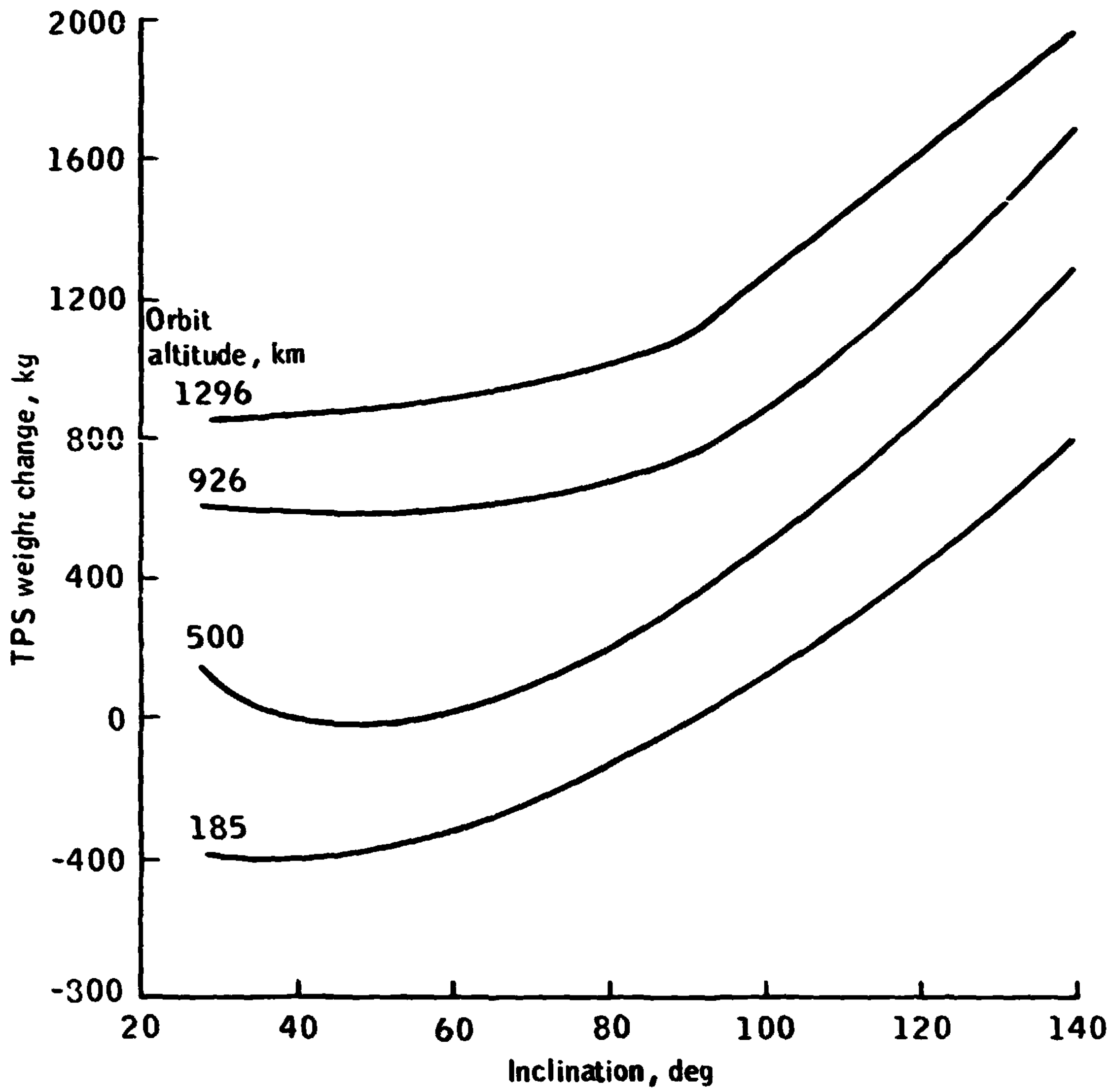

Figure 7.- Change in TPS weight as a function of inclination (angle of attack, 30°; nominal range).

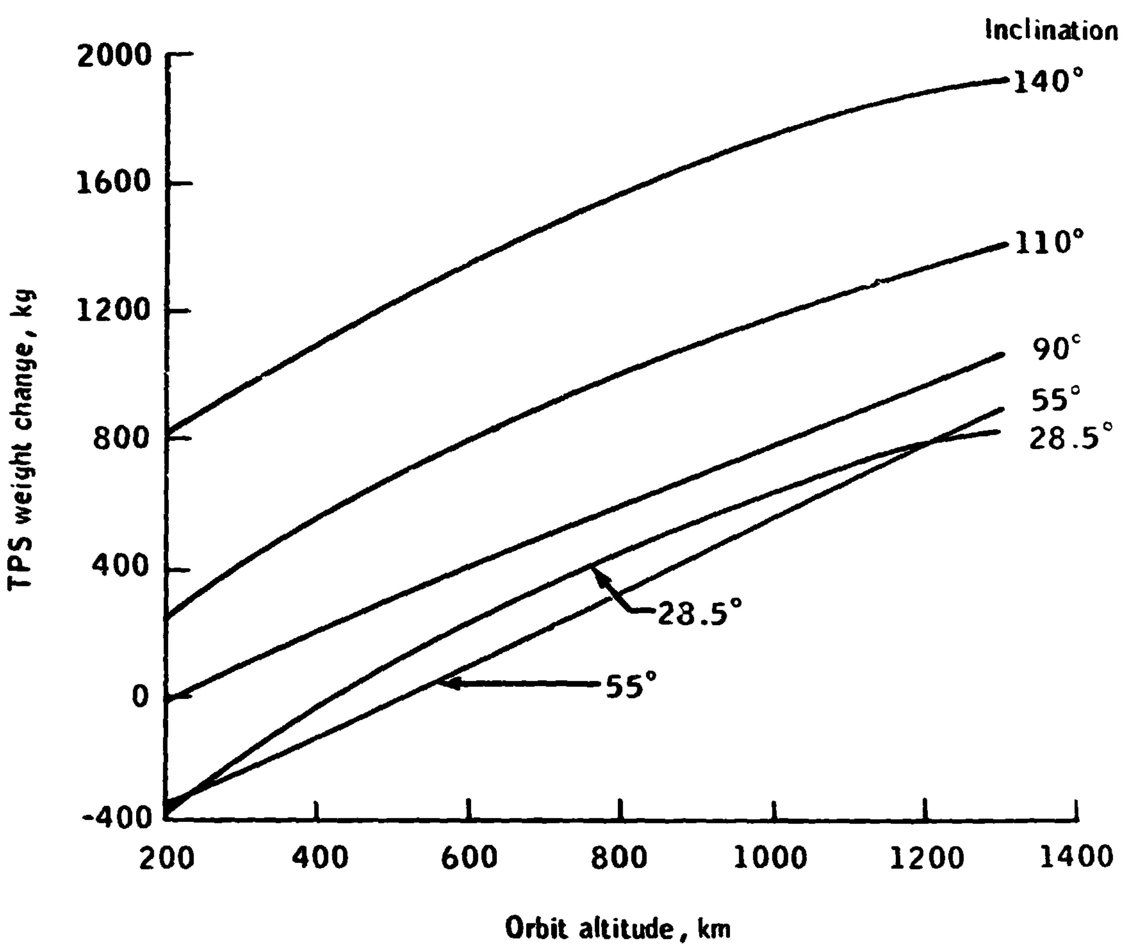

Figure 8.- Change in TPS weight as a fur^tion of deorbit apogee altitude (angle of attack, 30°; nominal range).

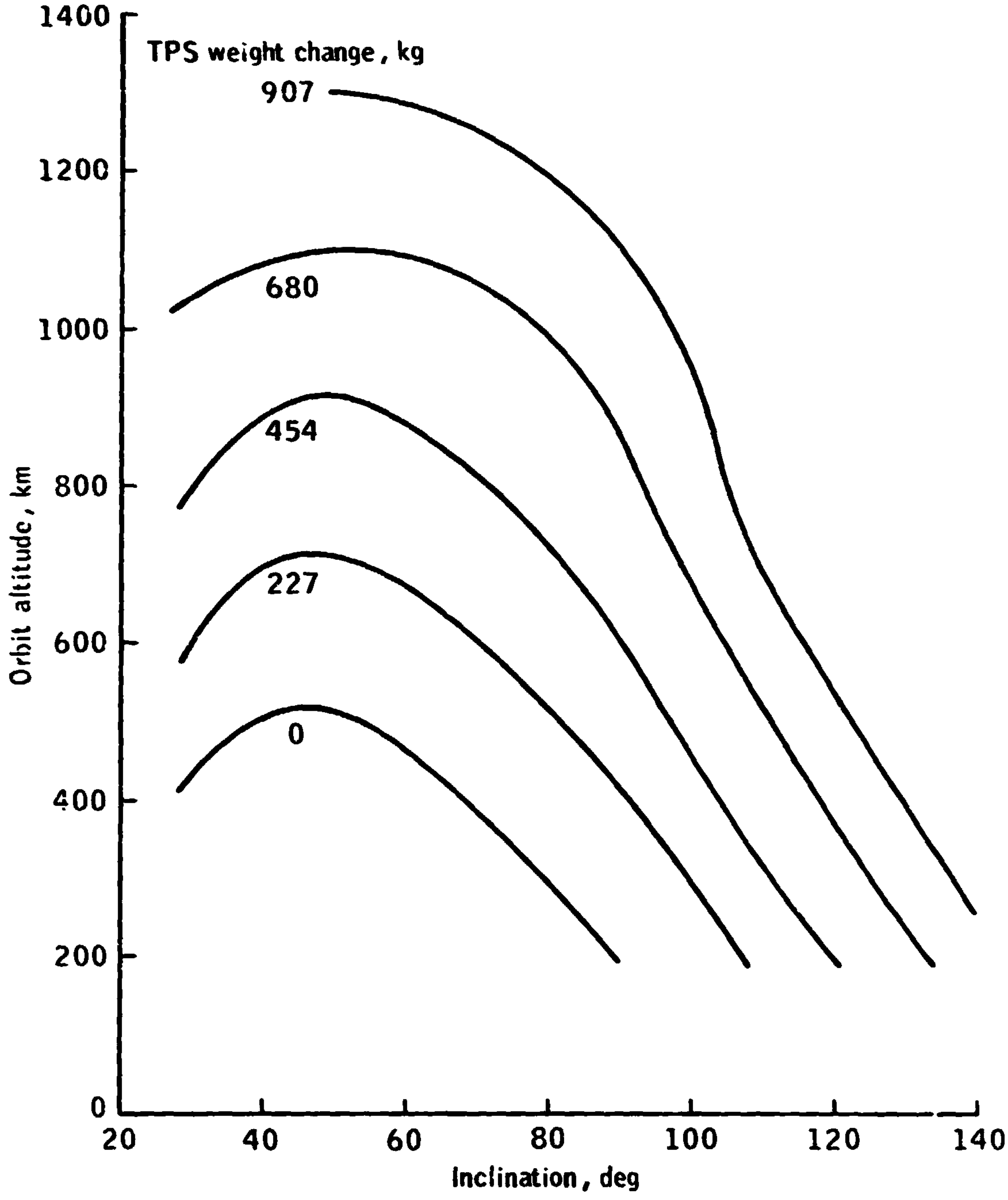

Figure 9.- The TPS weight change as a function of orbit altitude and inclination.

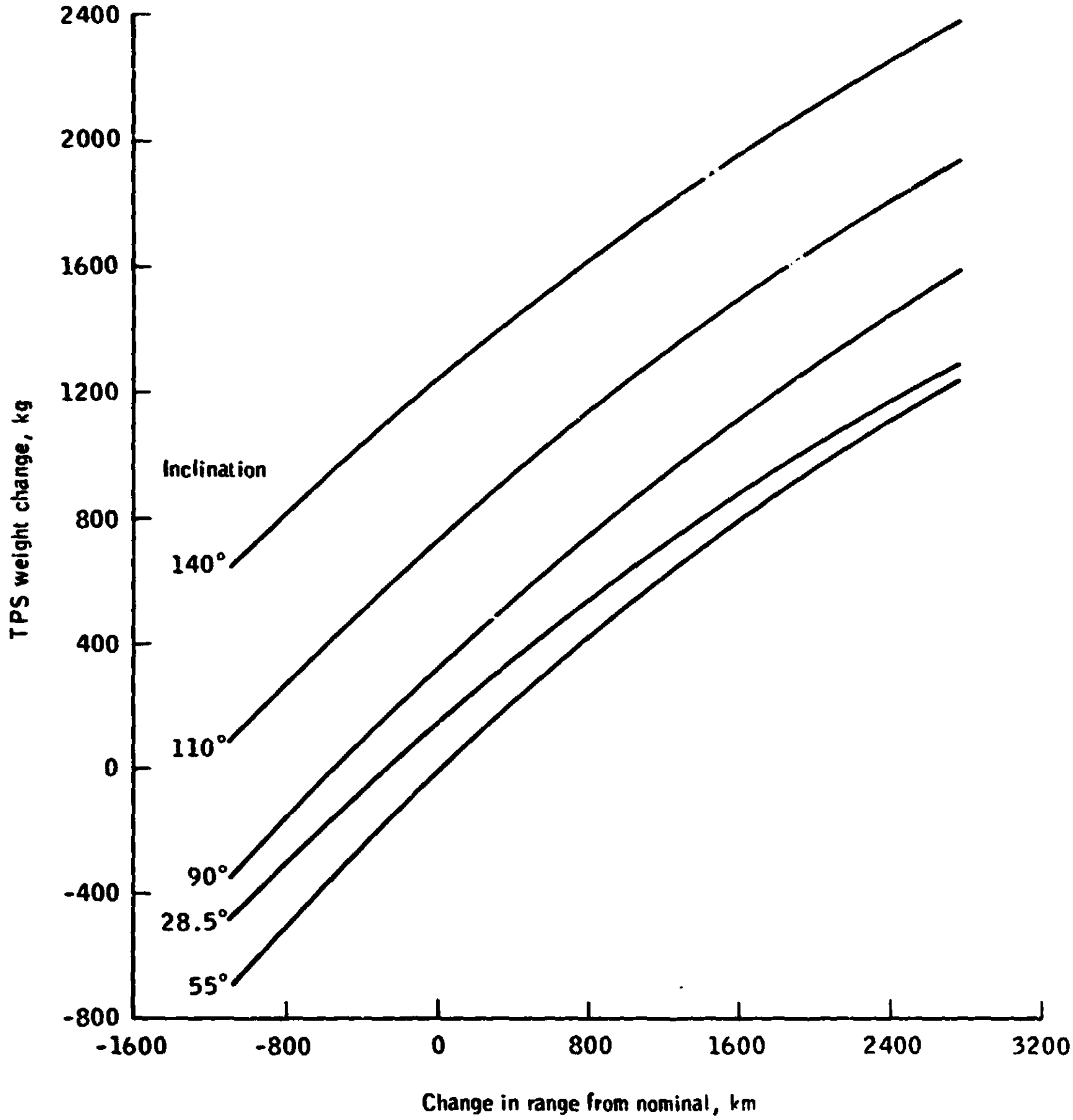

Figure 10.- Change in TPS weight as a function of range deviation from nominal range (angle of attack, 30°; orbit altitude, 500 kilometers).

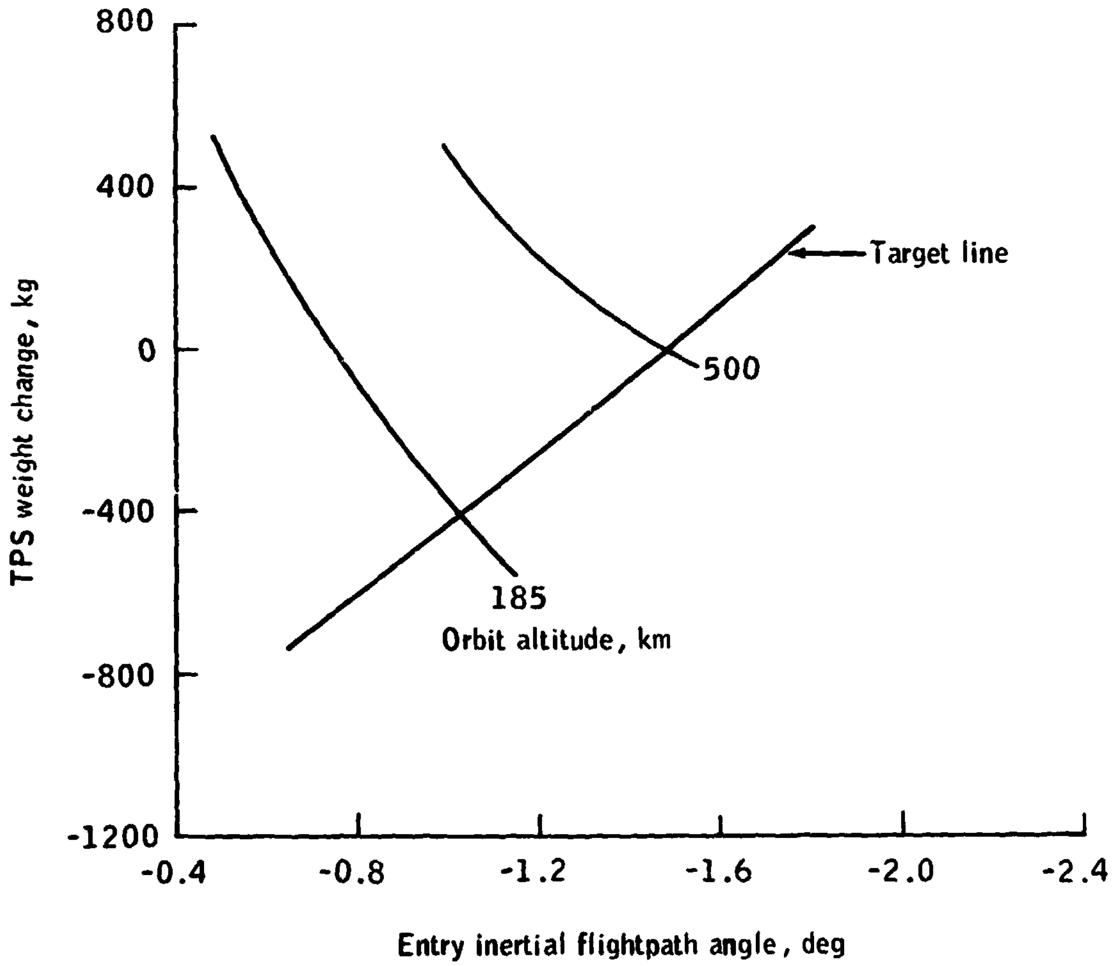

Figure 11.- Change in TPS weight as a function of entry inertial flightpath angle (inclination, 55°; angle of attack, 30°; nominal range).

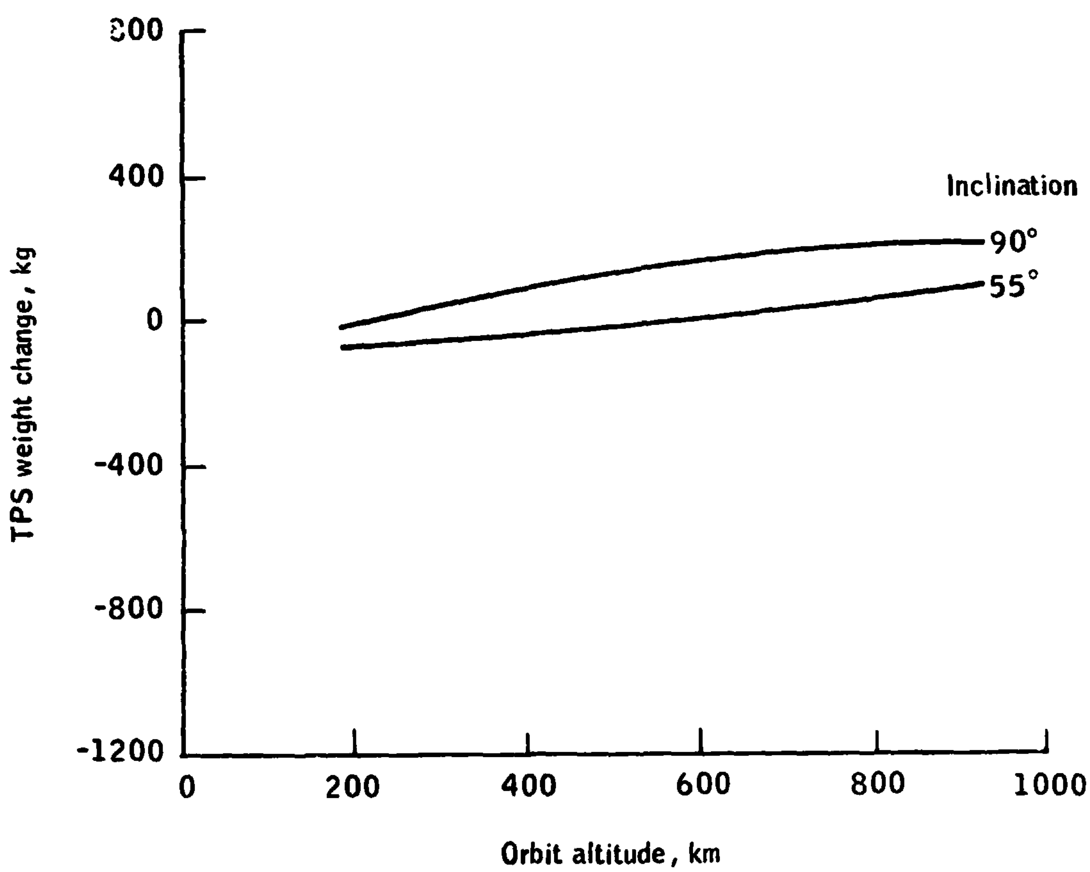

Figure 12.- Change in TPS weight as a function of orbit altitude (variable angle of attack, nominal range).

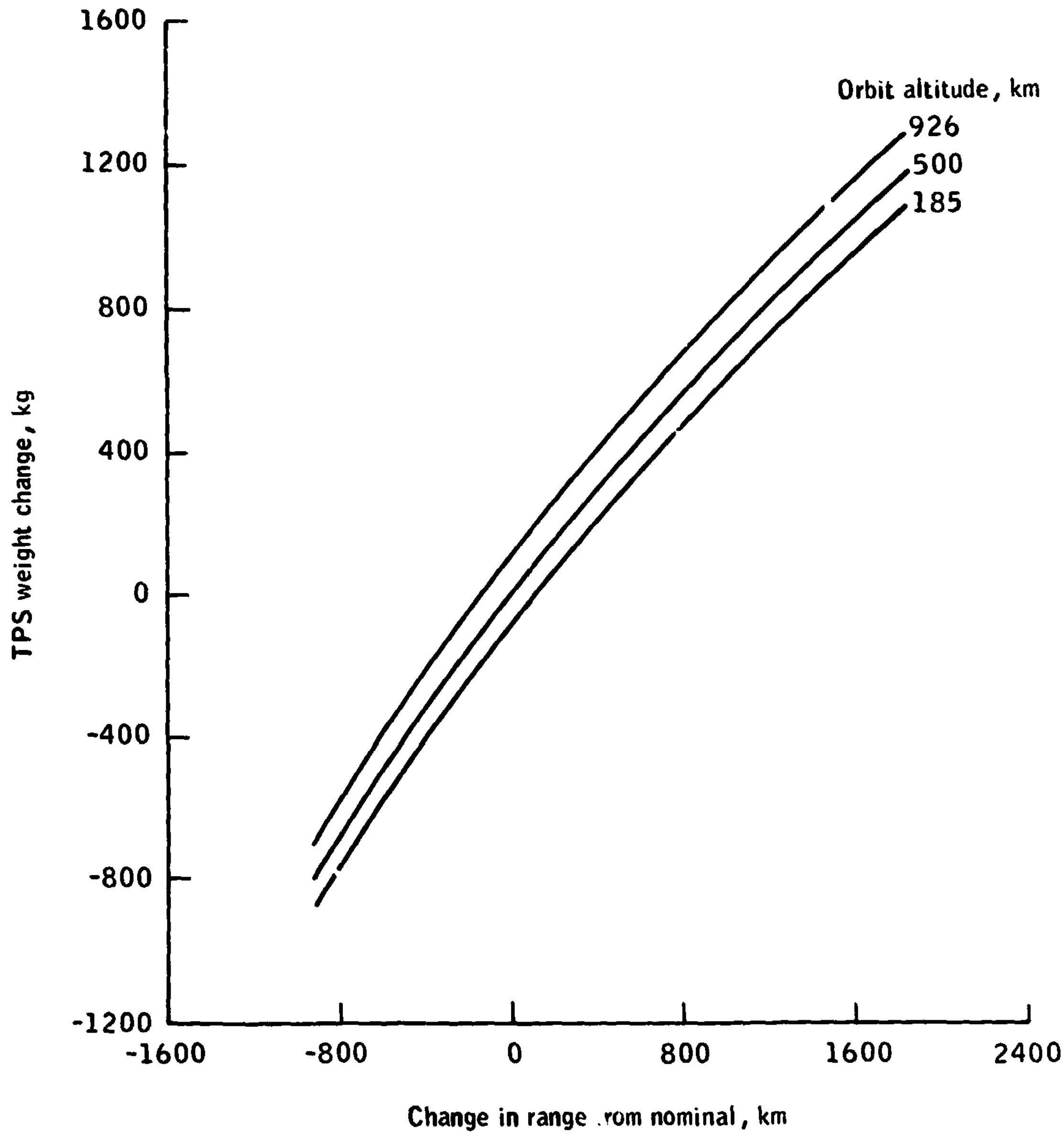

(a) Inclination, 55°.

Figure 13.- Change in TPS weight as a function of the orbit altitude and the range deviation from nominal range (variable angle of attack).

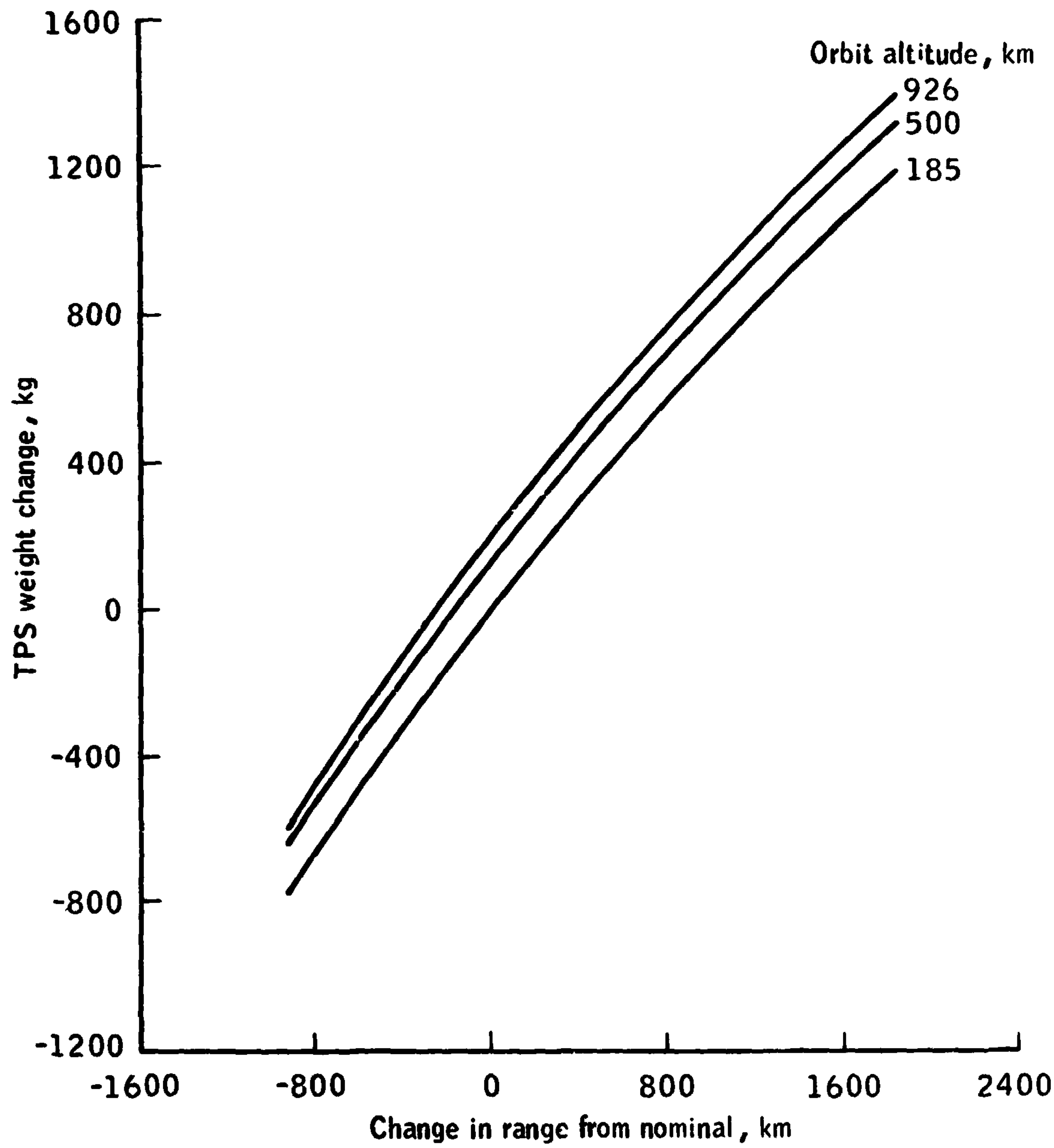

(b) Inclination, 90°.

Figure 13.- Concluded.

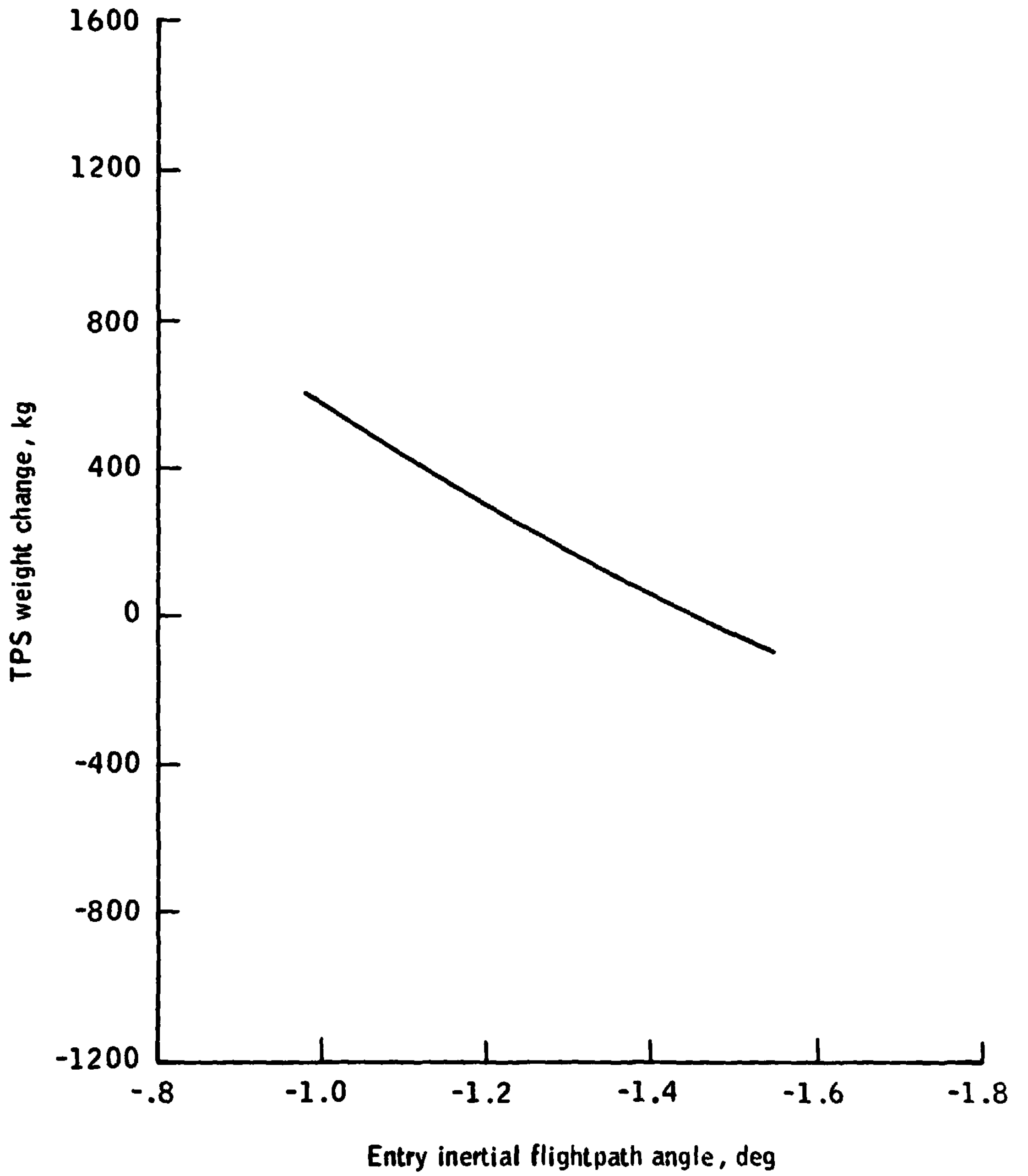

Figure 14.- Change in TPS weight as a function of entry inertial flightpath angle for a variable angle of attack (inclination, 55°; orbit altitude, 500 kilometers).